Abdominal Radiology (2019) 44:2864–2873
https://doi.org/10.1007/s00261-019-02023-1

PELVIS

Extracapsular extension on MRI indicates a more aggressive cell cycle progression genotype of prostate cancer

Andreas G. Wibmer[1] · Nicola L. Robertson[1] · Hedvig Hricak[1] · Junting Zheng[2] · Marinela Capanu[2] · Steven Stone[3] · Behfar Ehdaie[4] · Michael K. Brawer[5] · Hebert Alberto Vargas[1]

Published online: 27 April 2019

Abstract

Purpose To explore associations between magnetic resonance imaging (MRI) features of prostate cancer and expression levels of cell cycle genes, as assessed by the Prolaris® test.

Materials and methods Retrospective analysis of 118 PCa patients with genetic testing of biopsy specimen and prostate MRI from 08/2013 to 11/2015. Associations between the cell cycle risk (CCR) score and MRI features [i.e., PI-RADSv2 score, extracapsular extension (ECE), quantitative metrics] were analyzed with Fisher's exact test, nonparametric tests, and Spearman's correlation coefficient. In 41 patients (34.7%), test results were compared to unfavorable features on prostatectomy specimen (i.e., Gleason group ≥ 3, ECE, lymph node metastases).

Results Fifty-four (45.8%), 60 (50.8%), and 4 (3.4%) patients had low-, intermediate-, and high-risk cancers according to American Urological Association scoring system. Patients with ECE on MRI had significantly higher mean CCR scores (reader 1: 3.9 vs. 3.2, $p = 0.015$; reader 2: 3.6 vs. 3.2, $p = 0.045$). PI-RADSv2 scores and quantitative MRI features were not associated with CCR scores. In the prostatectomy subset, ECE on MRI ($p = < 0.001$–0.001) and CCR scores ($p = 0.049$) were significantly associated with unfavorable histopathologic features.

Conclusion The phenotypic trait of ECE on MRI indicates a more aggressive genotype of prostate cancer.

Keywords Prostate cancer · Risk assessment · Cell cycle progression gene expression · Magnetic resonance imaging · Radiogenomics

Introduction

The management of localized prostate cancer (PCa) hinges on the risk of disease progression that needs to be counterbalanced against the patient's overall fitness, life expectancy, and possible implications of cancer treatment. The American Urologic Association (AUA) guidelines base risk assessment on digital rectal examination, serum prostate-specific antigen (PSA) level, and PCa differentiation and abundance on prostate biopsy specimen. The specific strength of this algorithm lies in the identification of patients at low risk for disease progression who could be safely managed conservatively through active surveillance. Outcomes in patients classified as 'intermediate' risk, however, are heterogeneous with reported rates of 5-year disease progression ranging between 21 and 91% in a recent systematic review [1]. Several approaches have been pursued to further increase the accuracy and customization of risk stratification algorithms, including numerical risk

Electronic supplementary material The online version of this article (https://doi.org/10.1007/s00261-019-02023-1) contains supplementary material, which is available to authorized users.

✉ Andreas G. Wibmer
wibmera@mskcc.org

[1] Department of Radiology, Memorial Sloan Kettering Cancer Center, 1275 York Avenue, New York, NY 10065, USA

[2] Department of Epidemiology and Biostatistics, Memorial Sloan Kettering Cancer Center, New York, NY, USA

[3] Myriad Genetics, Salt Lake City, UT, USA

[4] Department of Surgery, Urology Service, Memorial Sloan Kettering Cancer Center, New York, NY, USA

[5] MDX Health, Irvine, CA, USA

scores [2], nomograms [3], as well as blood and genomic biomarkers [4]. The Prolaris® genetic test (Myriad Genetics Inc, Salt Lake City, USA) measures the expression of 46 genes associated with cell cycle progression and cell division in PCa tissue. Its results are mathematically combined with a patient's Cancer of the Prostate Risk Assessment (CAPRA) score and summarized as a numeric 'cell cycle risk (CCR)' score, which allows for more accurate prognostication and thus more individualized management decisions [5].

Multiparametric magnetic resonance imaging (MRI) of the prostate is routinely used for diagnosis and staging [6, 7], biopsy planning [8], and management decision support [9]. Numerous studies have reported associations between a tumor's MRI appearance and histopathologic characteristics [10–13]; possible associations of a cancer's MR imaging phenotype and genetic profile, however, are less thoroughly studied [14, 15]. The aim of this study was to explore potential associations between comprehensive quantitative and qualitative MRI features and the Prolaris® CCR score.

Materials and methods

Study population

This institutional review board-approved, retrospective study included consecutive men with biopsy-proven prostate cancer, who underwent Prolaris® testing from August 2013 to November 2015. Men were included in the study if they met the following criteria: multiparametric 3 Tesla prostate MRI within 6 months of the genetic test, MRI performed at our institution using the protocol detailed below, and adequate biopsy tissue to perform the genetic test. 118 men met the criteria and were included in the study. No patients were excluded.

Multiparametric MRI

All images were acquired on a 3 Tesla scanner (Discovery MR750w or Signa HDXT, GE Healthcare), and consisted of axial T1-weighted (repetition time, 450–750 ms; echo time, 7–12 ms; section thickness, 5 mm; intersection gap, 1 mm; field of view, 28–36 cm; matrix, 256 × 256–512 × 512), high-resolution axial/coronal/sagittal T2-weighted sequences (repetition time, 2500–6500 ms; echo time, 100–120 ms; section thickness, 3–5 mm; intersection gap, 0–1 mm; field of view, 14–24 cm; matrix, 256 × 192–512 × 512), and diffusion-weighted imaging with multiple b values (repetition time, 3500–8500 ms; echo time, 60–100 ms; field of view, 16–20 cm; section thickness, 3–5 mm; intersection gap 0–1 mm; field of view 14–24 cm; matrix 256 × 256; b values between 0 and 1000 s/mm^2). Apparent diffusion coefficient (ADC) maps were generated from DWI using a monoexponential model. Two board-certified radiologists (N.L.R., A.G.W.) with 4 and 6 years of experience in interpreting prostate MRI, who were blinded to all clinical data and the patients' CCR scores, read all MRIs. Recorded MRI features, including PI-RADS version 2

Table 1 Recorded MRI features

Feature	Description	Range
PI-RADS score	According to the Prostate Imaging Reporting and Data System version 2	1–5
Extracapsular tumor extension (ECE)	Tumor spread beyond the prostate gland, assessed on a 5-point Likert scale; 1–3: absent, 4–5: present Criteria on MRI: capsular contact/abutment; loss of T2 hypointense capsule; capsular bulging, irregularity, and/or retraction; neurovascular bundle retraction and/or thickening; presence of measurable extraprostatic tumor tissue; obliteration of recto-prostatic angle	Absent/present
Maximal tumor diameter	Maximum diameter of a dominant lesion on T2-weighted images (any plane) and ADC maps, respectively. '0,' if no dominant lesion was present	Continuous
Mean ADC[a]	Mean ADC value of a dominant lesion; or, if no dominant lesion was present, mean ADC of normal appearing peripheral zone tissue	Continuous
Overall tumor volume[b]	Volume of the largest dominant lesion on ADC maps. '0,' if no dominant lesion was present	Continuous
Markedly diffusion restricted tumor volume[b]	Tumor volume with ADC < 1000 mm^2/s. '0,' if no dominant lesion was present	Continuous

[a]Region of interest (ROI) placed in the center of a dominant lesion being as large as possible, but remaining confined to the tumor margins to limit partial volume effects

[b]Measured with TeraRecon® software. The reader contoured the outline of each tumor on every slice (free-hand), using the ADC map derived from the b-0-1000 DWI sequences. The histogram analysis tool was then applied, which calculated the volume of tumor within two pre-defined ADC bins (i.e., < 1000 and ≥ 1000 mm^2/s)

score [16], extracapsular tumor extension (ECE), and quantitative metrics, are listed in Table 1.

Prolaris® gene expression testing

All patients underwent systematic transrectal ultrasound-guided prostate biopsy, the number of systematic cores per patient was ≤ 10 ($n = 4$), 12 ($n = 57$), 14 ($n = 46$), or > 14 ($n = 11$). Thirty-seven patients (31.4%) also underwent targeted biopsy, the number of targeted cores ranged between one to four. The Prolaris® test (Myriad Genetics Inc, Salt Lake City, UT, USA) was applied to biopsy specimens performed at our institution in all study subjects. The test measures the expression level of 31 cell cycle progression (CCP) genes and 15 housekeeper genes to generate a CCP score [17]. The CCP score is mathematically combined using a validated algorithm with the patient's CAPRA score (13), resulting in the CCR score. Each 1-unit increase in CCR score represents a doubling of risk for PCa-specific mortality, with a higher score representing more aggressive cancers. Furthermore, the test result reports an individual patient's relative risk compared to other patients within the same AUA risk category (i.e., "less aggressive," "consistent," or "more aggressive" than the average patient within the same AUA risk category). A subgroup analysis of patients undergoing radical prostatectomy was performed to investigate the association of genetic test results and MRI features with unfavorable histopathologic features, i.e., Gleason group ≥ 3, ECE, lymph node metastases.

Statistical analysis

We examined associations of MRI features with the genetic test results and AUA risk group in all patients, and of MRI features with unfavorable findings on prostatectomy specimen using Fisher's exact test, exact Wilcoxon rank-sum test, and exact Kruskal–Wallis test. Spearman's correlation coefficient was estimated between CCR and continuous tumor length or volume on MRI. The bias-corrected 95% confidence intervals (CI) for correlation coefficients were estimated using nonparametric bootstrapping method with 2000 replicates. Agreement was assessed using kappa (or weighted kappa with squared weights) on categorical features, intraclass correlation coefficients (ICC), and limits of agreement on continuous variables. The bias-corrected 95% CI were estimated for kappa and ICC.

Results

The study population consisted of 118 men with a mean age of 61.4 ± 7.4 years. According to the AUA criteria, 54 (45.8%) men were classified as low-risk, 60 (50.8%) as intermediate, and 4 (3.4%) as high-risk patients. The median CCR score was 3.3 (range 1.6–5.5). In 57 (48.3%) patients, the genetic relative risk was "consistent" with the average, while 33 (28.0%) had "less aggressive" PCa, and 28 (23.7%) had "more aggressive" disease than the average within the same AUA category. On MRI, no patient was classified as PI-RADS 1, while a PI-RADS score of 2, 3, 4, and 5 was assigned in 21 and 20 (17.8% and 16.9%), 32 and 38 (27.1% and 32.2%), 53 and 52 (44.9% and 44.1%), and 12 and 8 (10.2% and 6.8%) cases by reader 1 and 2, respectively; inter-reader agreement for PI-RADS scores was moderate (kappa 0.789). ECE was deemed present in 20 (16.9%) patients by reader 1, and in 18 (15.3%) cases by reader 2; inter-reader agreement for ECE on MRI was strong (kappa 0.81). Detailed descriptive statistics for all metric MRI-derived variables (i.e., tumor length on T2-weighted images and ADC maps, mean ADC, tumor volumes) including inter-reader agreement statistics are provided in Supplement Table 1.

Association between AUA risk categorization and MRI features

Higher AUA risk categorization was significantly associated with higher PI-RADS scores ($p < 0.001$ for both readers), a higher likelihood of having ECE on MRI ($p < 0.001$ for both readers) and larger tumor diameters on T2-weighted images ($p = 0.002$–0.004) and ADC maps ($p = 0.002$–0.004). Also, mean tumor volume on ADC maps ($p = 0.002$ for both readers) and the volume of markedly diffusion restricted tumor volume ($p = 0.001$–0.002) were higher in higher AUA risk categories. Higher AUA risk categorization was also associated with lower mean ADC values ($p = 0.007$–0.008). Detailed numbers of these analyses are given in Supplement Table 2.

Association between MRI features and genetic test results

As detailed in Table 2 and Fig. 1, there was a significant association of the CCR score and the presence of ECE on MRI (reader 1: $p = 0.015$, reader 2: 0.045), while there were no significant associations observed between CCR score and PI-RADS score or any of the quantitative MRI features. As listed in Table 3, there was no significant association between the evaluated MRI features and the likelihood of the genetic test indicating "less aggressive" or "more aggressive" disease.

Associations with adverse histopathologic features

Of the 118 study subjects, 41 (34.7%) underwent radical prostatectomy, of which 18/41 (43.9%) were found to have

Table 2 Associations between MRI features and CCR score

Qualitative MRI features	Reader 1		Reader 2	
	Median CCR score (range)	*p*-value	Median CCR score (range)	*p*-value
PI-RADS v2 scores		0.289		0.214
2	2.9 (1.8, 5.5)		2.85 (1.8, 5.5)	
3	3.25 (2.1, 4.7)		3.3 (2, 4.7)	
4	3.3 (2.2, 4.7)		3.3 (1.6, 4.7)	
5	3.75 (1.6, 4.6)		3.75 (2.6, 4.6)	
Extracapsular extension		0.015		0.045
Absent	3.2 (1.6, 5.5)		3.2 (1.6, 5.5)	
Present	3.9 (2.3, 4.6)		3.6 (2.3, 4.6)	
Quantitative MRI features	Correlation coefficient with (95% CI)	*p*-value	Correlation coefficent with (95% CI)	*p*-value
Tumor length on T2w images	0.127 (−0.049, 0.314)	0.169	0.105 (−0.074, 0.29)	0.257
Tumor length on ADC maps	0.117 (−0.068, 0.298)	0.207	0.084 (−0.101, 0.268)	0.368
Tumor volume on ADC maps	0.132 (−0.049, 0.318)	0.154	0.136 (−0.045, 0.321)	0.143
Tumor ADC value	−0.154 (−0.33, 0.046)	0.096	−0.106 (−0.279, 0.083)	0.254
Tumor volume with markedly restricted diffusion	0.144 (−0.036, 0.324)	0.120	0.173 (−0.014, 0.356)	0.061

ADC apparent diffusion coefficient, *AUA* American Urologic Association, *CCR* cell cycle risk, *PI-RADSv2* Prostate Imaging Reporting and Data System version 2

at least one unfavorable finding on surgical histopathology (i.e., Gleason score 4 + 3 or higher in 9, ECE in 15, lymph node metastases in 5 patients). We observed significant associations of unfavorable surgical histopathology findings with the CCR score ($p = 0.049$), and the presence of ECE on MRI (reader 1: $p < 0.001$, reader 2: $p = 0.001$). We found a significant association of PI-RADS scores and unfavorable pathology features for reader 1 ($p = 0.036$), but not for reader 2 ($p = 0.779$). No significant associations were observed between unfavorable pathology features and patients' AUA risk category or any of the quantitative MRI features. Detailed numbers of these analyses are provided in Table 4, representative case studies are presented in Fig. 2.

Discussion

In this study, we explored associations between qualitative and quantitative prostate MRI features and the results of the Prolaris® genetic test in patients with low-, intermediate-, and high-risk PCa. The presence of ECE on MRI was associated with a higher CCR score. We did not find significant associations of the PI-RADS score or quantitative MRI features with the results of the genetic test. Renard-Penna et al. have previously analysed possible associations between (semi-)quantitative MRI features and cell cycle gene expression in prostate cancer [14, 15]. In concordance with our results, they did not find an association of tumor size and gene expression profile. For tumor ADC values, they reported a significant association with the CCP score in a cohort of 106 patients [15], but could not find this association in another cohort of 67 men [14], the latter being in concordance with our results. When assessed on a 5-point Likert scale [14], the cell cycle progression score was not associated with the MRI appearance of prostate cancer. However, when applying a 15-point scale derived from the PI-RADS version 1 classification algorithm, the authors found a significant association with the CCP score [15]. In neither of these studies, the authors evaluated the presence of ECE on MRI, which was associated with cell cycle gene expression in our cohort. In our subgroup analysis of patients undergoing prostatectomy, the CCR score and the presence of ECE on MRI were associated with unfavorable histopathologic features on prostatectomy specimen.

The Prolaris® genetic test measures the expression of 31 genes associated with cell cycle progression and cell division, as well as 15 housekeeping genes in prostate cancer tissue specimen. Its results are represented by a proliferative index, expressed as 'cell cycle progression' score, which is then mathematically combined with a patient's CAPRA score and summarized as a numeric CCR score. The prognostic potential of this test has been evaluated in

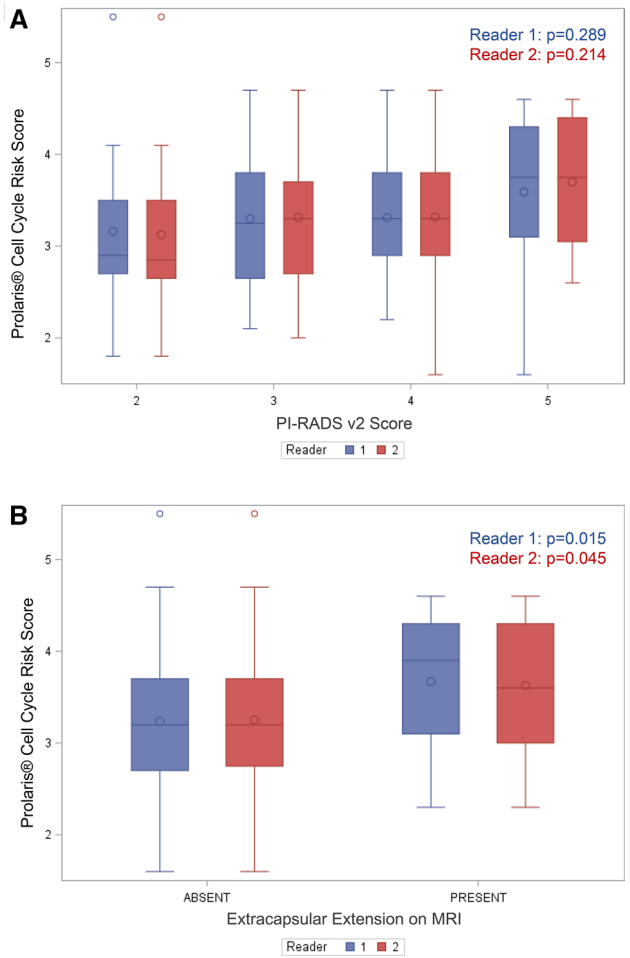

Fig. 1 Distribution of the cell cycle risk score among PI-RADSv2 scores (**a**), and among patients with and without extracapsular extension on MRI (**b**), respectively; data are shown separately for reader 1 (blue) and reader 2 (red)

tissue specimen from transurethral resections [18], prostate biopsies [19], and prostatectomy specimen [20], and in regard to different clinical endpoints, including biochemical recurrence after prostatectomy [21] and radiation therapy [22], development of metastases [20], and mortality [23]. The potential of prostate MRI features for predicting biochemical tumor recurrence have been suggested in the post-prostatectomy [24, 25] and post-radiotherapy [26] settings; in the latter two studies, the presence of ECE was associated with a higher likelihood of biochemical recurrence, independently of the cancer's Gleason grade and pre-treatment PSA levels, respectively [25, 26]. The present study provides one possible molecular foundation for the poor prognostic implications of ECE on MRI. Both the genetic test results and the presence of ECE on MRI are associated with a higher risk of tumor recurrence after treatment, thus it will be interesting to assess the combined ability of these tools for prognostication in patients with prostate cancer. Theoretically, MRI might provide macroscopic phenotypic information and be less affected by sampling bias and genetic tumor heterogeneity [27], while the genomic test could compensate for some limitations of MRI, e.g., limited sensitivity for low-volume and/or low-grade malignancy [28], artifact and distortion [29], and inter-observer variability [30]. Due to the short follow-up period, the number of events (biochemical recurrence) limits statistical testing of this hypothesis in the current study.

Our study has several limitations, most importantly its retrospective design. By blinding the reader to all clinical data and the results of the genetic test, we aimed to minimize the probability of a confirmation bias. By including all consecutive patients undergoing genetic testing and prostate MRI, we tried to minimize selection bias; the relatively low proportion of patients with AUA high-risk disease indicates that the latter might still be present. Also, we were not able to objectively assess the indication for genetic testing to incorporate into our analysis, which is a possible additional source of selection bias. At our institution, men with newly diagnosed prostate cancer routinely undergo MRI for staging, risk stratification, and treatment planning, decreasing the likelihood that the indication for MRI poses a substantial source of bias in this study. The lack of histopathological prove for tumor length, tumor volume, and presence of ECE in patients not undergoing prostatetctomy is another limitation of our study. Due to the small number of patients undergoing prostatectomy, we were not able to conduct multivariate statistical modeling to directly compare MRI and genetic features in their ability to predict unfavorable pathology features.

Conclusion

The phenotypic trait of extraprostatic tumor extension on MRI indicates a more aggressive genotype of prostate cancer, as quantified by the Prolaris® cell cycle risk score. Extracapsular extension on MRI and the genetic test result are associated with adverse histopathologic features on prostatectomy specimen.

Table 3 Associations between MRI features and Prolaris® relative risk

MRI features	Reader 1			*p*-value	Reader 2			*p*-value
	Prolaris® relative risk				Prolaris® relative risk			
	Less aggressive ($n=33$)	Consistent ($n=57$)	More aggressive ($n=28$)		Less aggressive ($n=33$)	Consistent ($n=57$)	More aggressive ($n=28$)	
PI-RADS v2 scores				0.475				0.617
2	7 (21.2)	10 (17.5)	4 (14.3)		8 (24.2)	8 (14.0)	4 (14.3)	
3	11 (33.3)	12 (21.1)	9 (32.1)		12 (36.4)	16 (28.1)	10 (35.7)	
4	13 (39.4)	30 (52.6)	10 (35.7)		12 (36.4)	29 (50.9)	11 (39.3)	
5	2 (6.1)	5 (8.8)	5 (17.9)		1 (3.0)	4 (7.0)	3 (10.7)	
Extracapsular extension (%)	3 (9.1)	8 (14.0)	9 (32.1)	0.054	4 (12.1)	8 (14.0)	9 (32.1)	0.300
Median tumor length on T2w images (mm) [range]	7.0 [0.0, 25.4]	8.5 [0.0, 23.2]	8.7 [0.0, 35.4]	0.468	6.1 [0.0, 26.8]	7.8 [0.0, 25.3]	8.3 [0.0, 30.9]	0.729
Median tumor length on ADC maps (mm) [range]	6.0 [0.0, 27.8]	8.7 [0.0, 26.0]	7.6 [0.0, 36.4]	0.462	6.2 [0.0, 27.0]	7.8 [0.0, 24.6]	6.8 [0.0, 37.1]	0.546
Median tumor volume on ADC maps (cm^3) [range]	0.1 [0.0, 3.9]	0.3 [0.0, 4.9]	0.2 [0.0, 8.9]	0.368	0.1 [0.0, 0.6]	0.3 [0.0, 0.8]	0.2 [0.0, 0.9]	0.245
Median tumor ADC values (mm^2/s) [range]	1.2 [0.4, 1.9]	1.0 [0.5, 2.5]	1.0 [0.4, 1.9]	0.223	1.2 [0.9, 1.5]	0.9 [0.8, 1.5]	1.0 [0.7, 1.5]	0.491
Median tumor volume with markedly restricted diffusion (cm^3) [range]	0.0 [0.0, 3.5]	0.1 [0.0, 3.3]	0.0 [0.0, 7.5]	0.287	0.0 [0.0, 0.2]	0.10 [0.0, 0.5]	0.10 [0.0, 0.5]	0.144

ADC apparent diffusion coefficient, *PI-RADSv2* Prostate Imaging Reporting and Data System version 2

Table 4 Associations of MRI features and unfavorable findings on prostatectomy histopathology

Variable	No adverse feature ($n=23$)	Any adverse feature ($n=18$)	p-value
AUA risk (%)			
High	0 (0.0)	2 (11.1)	0.161
Intermediate	13 (56.5)	12 (66.7)	
Low	10 (43.5)	4 (22.2)	
Median CCR score [range]			
Prolaris® results	3.1 [2.2, 5.5]	3.8 [1.8, 4.7]	0.049
Relative risk (%)			0.311
Less aggressive	6 (26.1)	4 (22.2)	
Consistent	12 (52.2)	6 (33.3)	
More aggressive	5 (21.7)	8 (44.4)	

	Reader 1			Reader 2		
	No adverse feature ($n=23$)	Any adverse feature ($n=18$)	p-value	No adverse feature ($n=23$)	Any adverse feature ($n=18$)	p-value
Magnetic resonance imaging features						
PI-RADSv2 scores (%)			0.036			0.779
2	2 (8.7)	1 (5.6)		3 (13.0)	1 (5.6)	
3	6 (26.1)	5 (27.8)		7 (30.4)	5 (27.8)	
4	15 (65.2)	7 (38.9)		12 (52.2)	10 (55.6)	
5	0 (0)	5 (27.8)		1 (4.3)	2 (11.1)	
Extracapsular extension (%)	1 (4.3)	9 (50.0)	0.001	0 (0.0)	9 (50.0)	<0.001
Median tumor length on T2w images (mm) [range]	7.0 [0.0, 17.9]	11.1 [0.0, 29.3]	0.070	7.4 [0.0, 16.6]	11.2 [0.0, 26.8]	0.166
Median tumor length on ADC maps (mm) [range]	7.5 [0.0, 18.0]	11.6 [0.0, 28.1]	0.052	7.3 [0.0, 17.2]	10.6 [0.0, 27.0]	0.201
Median tumor volume on ADC maps (cm^3) [range]	0.28 [0.0, 3.51]	0.54 [0.0, 3.28]	0.293	0.26 [0.0, 3.38]	0.60 [0.0, 3.67]	0.253
Median tumor ADC values (mm^2/s) [range]	1.04 [0.6, 1.73]	0.89 [0.42, 1.87]	0.331	0.94 [0.58, 1.9]	0.95 [0.42, 1.88]	0.854
Median tumor volume with markedly restricted diffusion (cm^3) [range]	0.07 [0.0, 2.26]	0.21 [0.0, 2.88]	0.125	0.10 [0.0, 2.23]	0.15 [0.0, 3.25]	0.255

ADC apparent diffusion coefficient, *AUA* American Urologic Association, *CCR* cell cycle risk, *PI-RADSv2* Prostate Imaging Reporting and Data System version 2

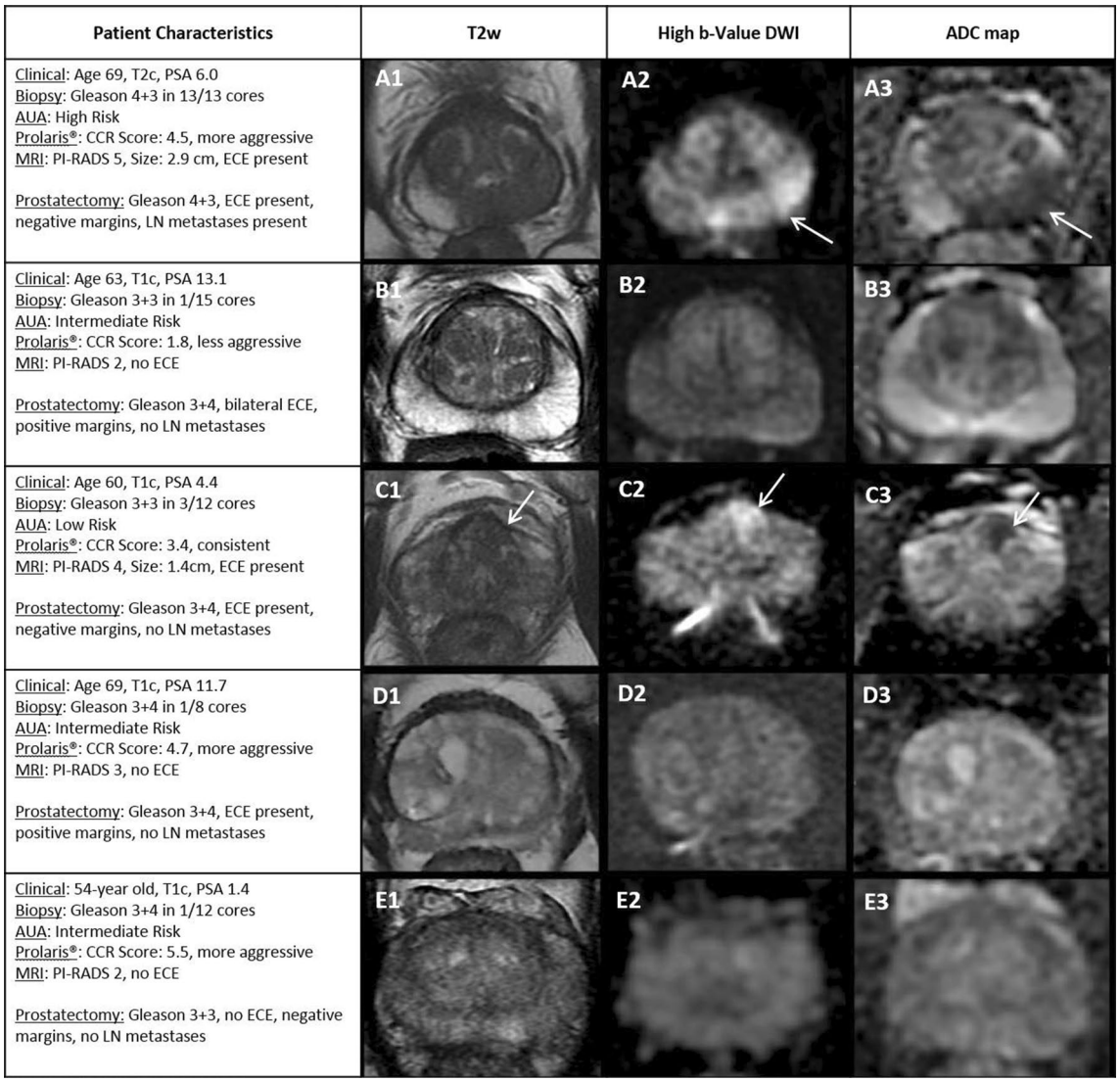

Fig. 2 Representative T2-weighted images (T2w, column 1), high b value diffusion-weighted images (DWI, column 2), and apparent diffusion coefficient maps (ADC, column 3) of 5 patients (**a**–**e**), which highlight the strengths and imperfections of the investigated risk assessment tools, i.e., AUA criteria, Prolaris® test, and MRI. Patient A: concordant high-risk features by AUA criteria, genetic test, and MRI (arrow indicates a dominant lesion in the left posterior peripheral zone with ECE); high-grade cancer with unfavorable features was verified on surgical histopathology. Patient B: PSA 13.1 ng/ml, otherwise low-risk features on clinical examination, biopsy, genetic test, and MRI (no measurable lesion); surgical histopathology showed ECE and positive surgical margins. Patient C: low-risk features by AUA criteria and the genetic test, MRI showed an anterior lesion with ECE (white arrows), which was verified on the surgical specimen. Patient D: intermediate risk by AUA criteria with more aggressive gene expression profile on the genetic test, MRI was equivocal for a measurable lesion and did not show ECE; surgical pathology revealed ECE and positive surgical margins. Patient E: Intermediate risk by AUA criteria with more aggressive gene expression profile on the genetic test, MRI was negative for a measurable lesion or ECE; low-grade tumor without unfavorable features on the prostatectomy specimen

Compliance with ethical standards

Conflict of interest Steve Stone is an employee of Myriad Genetics, Salt Lake City, UT, USA. Michael K Brawer is a former employee of Myriad Genetics, Salt Lake City, UT, USA. Andreas G Wibmer was supported by the Peter Michael Foundation.

References

1. Kane CJ, Eggener SE, Shindel AW, Andriole GL (2017) Variability in Outcomes for Patients with Intermediate-risk Prostate Cancer (Gleason Score 7, International Society of Urological Pathology Gleason Group 2-3) and Implications for Risk Stratification: A Systematic Review. Eur Urol Focus. https://doi.org/10.1016/j.euf.2016.10.010
2. Cooperberg MR, Pasta DJ, Elkin EP et al (2005) The University of California, San Francisco Cancer of the Prostate Risk Assessment score: a straightforward and reliable preoperative predictor of disease recurrence after radical prostatectomy. J Urol 173:1938-1942
3. Touijer K, Scardino PT (2009) Nomograms for staging, prognosis, and predicting treatment outcomes. Cancer 115:3107-3111
4. Lamy PJ, Allory Y, Gauchez AS et al (2017) Prognostic Biomarkers Used for Localised Prostate Cancer Management: A Systematic Review. Eur Urol Focus. https://doi.org/10.1016/j.euf.2017.02.017
5. Moschini M, Spahn M, Mattei A, Cheville J, Karnes RJ (2016) Incorporation of tissue-based genomic biomarkers into localized prostate cancer clinics. BMC Med 14:67
6. Taghipour M, Ziaei A, Alessandrino F et al (2018) Investigating the role of DCE-MRI, over T2 and DWI, in accurate PI-RADS v2 assessment of clinically significant peripheral zone prostate lesions as defined at radical prostatectomy. Abdom Radiol (NY). https://doi.org/10.1007/s00261-018-1807-6
7. Mathur S, O'Malley ME, Ghai S et al (2018) Correlation of 3T multiparametric prostate MRI using prostate imaging reporting and data system (PIRADS) version 2 with biopsy as reference standard. Abdom Radiol (NY). https://doi.org/10.1007/s00261-018-1696-8
8. Campa R, Del Monte M, Barchetti G et al (2018) Improvement of prostate cancer detection combining a computer-aided diagnostic system with TRUS-MRI targeted biopsy. Abdom Radiol (NY). https://doi.org/10.1007/s00261-018-1712-z
9. Tamada T, Dani H, Taneja SS, Rosenkrantz AB (2017) The role of whole-lesion apparent diffusion coefficient analysis for predicting outcomes of prostate cancer patients on active surveillance. Abdom Radiol (NY) 42:2340-2345
10. Alessandrino F, Taghipour M, Hassanzadeh E et al (2018) Predictive role of PI-RADSv2 and ADC parameters in differentiating Gleason pattern 3 + 4 and 4 + 3 prostate cancer. Abdom Radiol (NY). https://doi.org/10.1007/s00261-018-1718-6
11. Holtz JN, Silverman RK, Tay KJ et al (2018) New prostate cancer prognostic grade group (PGG): Can multiparametric MRI (mpMRI) accurately separate patients with low-, intermediate-, and high-grade cancer? Abdom Radiol (NY) 43:702-712
12. Glazer DI, Hassanzadeh E, Fedorov A et al (2017) Diffusion-weighted endorectal MR imaging at 3T for prostate cancer: correlation with tumor cell density and percentage Gleason pattern on whole mount pathology. Abdom Radiol (NY) 42:918-925
13. Shaish H, Kang SK, Rosenkrantz AB (2017) The utility of quantitative ADC values for differentiating high-risk from low-risk prostate cancer: a systematic review and meta-analysis. Abdom Radiol (NY) 42:260-270
14. Renard Penna R, Cancel-Tassin G, Comperat E et al (2016) Apparent diffusion coefficient value is a strong predictor of unsuspected aggressiveness of prostate cancer before radical prostatectomy. World J Urol 34:1389-1395
15. Renard-Penna R, Cancel-Tassin G, Comperat E et al (2015) Multiparametric Magnetic Resonance Imaging Predicts Postoperative Pathology but Misses Aggressive Prostate Cancers as Assessed by Cell Cycle Progression Score. J Urol 194: 1617-1623
16. Hassanzadeh E, Glazer DI, Dunne RM, Fennessy FM, Harisinghani MG, Tempany CM (2017) Prostate imaging reporting and data system version 2 (PI-RADS v2): a pictorial review. Abdom Radiol (NY) 42:278-289
17. Warf M, Reid J, Brown K, Kimbrell H, Kolquist K (2015) Analytical Validation of a Cell Cycle Progression Signature Used as a Prognostic Marker in Prostate Cancer. J Mol Biomark Diagn 5:239
18. Cuzick J, Swanson GP, Fisher G et al (2011) Prognostic value of an RNA expression signature derived from cell cycle proliferation genes in patients with prostate cancer: a retrospective study. Lancet Oncol 12:245-255
19. Cuzick J, Berney DM, Fisher G et al (2012) Prognostic value of a cell cycle progression signature for prostate cancer death in a conservatively managed needle biopsy cohort. Br J Cancer 106:1095-1099
20. Bishoff JT, Freedland SJ, Gerber L et al (2014) Prognostic utility of the cell cycle progression score generated from biopsy in men treated with prostatectomy. J Urol 192:409-414
21. Cooperberg MR, Simko JP, Cowan JE et al (2013) Validation of a cell-cycle progression gene panel to improve risk stratification in a contemporary prostatectomy cohort. J Clin Oncol 31:1428-1434
22. Freedland SJ, Gerber L, Reid J et al (2013) Prognostic utility of cell cycle progression score in men with prostate cancer after primary external beam radiation therapy. Int J Radiat Oncol Biol Phys 86:848-853
23. Cuzick J, Stone S, Fisher G et al (2015) Validation of an RNA cell cycle progression score for predicting death from prostate cancer in a conservatively managed needle biopsy cohort. Br J Cancer 113:382-389
24. Tan N, Shen L, Khoshnoodi P et al (2017) Pathological and 3 Tesla Volumetric Magnetic Resonance Imaging Predictors of Biochemical Recurrence after Robotic Assisted Radical Prostatectomy: Correlation with Whole Mount Histopathology. J Urol. https://doi.org/10.1016/j.juro.2017.10.042
25. Rosenkrantz AB, Ream JM, Nolan P, Rusinek H, Deng FM, Taneja SS (2015) Prostate Cancer: Utility of Whole-Lesion Apparent Diffusion Coefficient Metrics for Prediction of Biochemical Recurrence After Radical Prostatectomy. AJR Am J Roentgenol 205:1208-1214
26. Fuchsjager MH, Pucar D, Zelefsky MJ et al (2010) Predicting post-external beam radiation therapy PSA relapse of prostate cancer using pretreatment MRI. Int J Radiat Oncol Biol Phys 78:743-750
27. Wei L, Wang J, Lampert E et al (2017) Intratumoral and Intertumoral Genomic Heterogeneity of Multifocal Localized Prostate Cancer Impacts Molecular Classifications and Genomic Prognosticators. Eur Urol 71:183-192
28. Mohammadian Bajgiran A, Afshari Mirak S, Shakeri S et al (2018) Characteristics of missed prostate cancer lesions on 3T multiparametric-MRI in 518 patients: based on PI-RADSv2 and using whole-mount histopathology reference. Abdom Radiol (NY). https://doi.org/10.1007/s00261-018-1823-6

29. Stocker D, Manoliu A, Becker AS et al (2018) Image Quality and Geometric Distortion of Modern Diffusion-Weighted Imaging Sequences in Magnetic Resonance Imaging of the Prostate. Invest Radiol 53:200-206
30. Sonn GA, Fan RE, Ghanouni P et al (2017) Prostate Magnetic Resonance Imaging Interpretation Varies Substantially Across Radiologists. Eur Urol Focus. https://doi.org/10.1016/j.euf.2017.11.010